

Characterization and calculation of energy levels scheme for $\text{Er}^{3+}:\text{ZnGa}_2\text{O}_4$

M. VASILE,^{a,b} N. AVRAM,^{a,c*} P. VLĂZAN^b, I. GROZESCU^b, M. MICLĂU^b

^aDepartment of Physics, West University of Timisoara, Timisoara, 300223, Romania

^bNational Institute for Research and Development in Electrochemistry and Condensed Matter, Timisoara, 300224, Romania

^cAcademy of Romanian Scientists, Bucharest, 050094, Romania

Zinc gallate (ZnGa_2O_4) is a normal spinal crystal structure, with Zn^{2+} ions in the tetrahedral sites and Ga^{3+} ions in the octahedral sites. ZnGa_2O_4 has attracted much attention due to its many possible applications for field emission display, electroluminescent devices and in the last mostly sensor domain. $\text{ZnGa}_2\text{O}_4:\text{Er}^{3+}$ nanoparticles were obtained by the hydrothermal method using Ga_2O_3 , $\text{Zn}(\text{NO}_3)_2 \cdot 6\text{H}_2\text{O}$ and Er_2O_3 precursors in basic medium using a Teflon-lined stainless steel autoclave tightly sealed. The near infrared photoluminescence study for the $\text{Er}^{3+}:\text{ZnGa}_2\text{O}_4$ nanocomposites showed a broad and strong emission band at 1550 nm which was attributed to the ${}^4\text{F}_{7/2} \rightarrow {}^4\text{I}_{15/2}$ transition of Er^{3+} ion..

(Received September 1, 2008; accepted October 30, 2008)

Keywords: Nanoparticles, $\text{ZnGa}_2\text{O}_4:\text{Er}^{3+}$, Hydrothermal method

1. Introduction

ZnGa_2O_4 phosphor has been used for low-voltage cathodoluminescence, vacuum fluorescent display and recently reported as a promising candidate for field emission displays. Among many oxide phosphors, zinc gallate (ZnGa_2O_4) is a normal spinal crystal structure which crystallizes in the cubic space group $\text{Fd}3\text{m}$ (O_h^7), with lattice constant $a=8.3358\text{\AA}$ [1], Zn^{2+} ions occupies octahedral sites and Ga^{3+} ions a tetrahedral sites or a trigonally distorted octahedral sites [2]. The unit cell contains 8 tetrahedral cations, 16 octahedral cations and 32 oxygen anions. The energy band gap of this crystal is about 4.4eV [3] and ZnGa_2O_4 shows blue photoluminescence without doping via transition of a self-activated center. ZnGa_2O_4 shows various emission colors when doped with some transitional metal or rare earth ions, such as Cr^{3+} , Mn^{2+} , Eu^{3+} or Ce^{3+} [4-8]. Synthesis of ZnGa_2O_4 spinel powders have been previously accomplished by traditional solid-state reactions between zinc oxide and gallium oxide [9-11] and by pulverizing ZnGa_2O_4 single crystals synthesized above 1000°C by the flux method [12,13]. As we know, different material preparation methods have some important effects on material microstructure and physical properties. In the recent decade, there is a strong trend toward the application of solution routes for direct synthesis of crystalline ceramic particles at low temperature [14, 15]. Hydrothermal method is one of the most promising solution chemical methods. The particles size and their distribution, phase homogeneity, and morphology could be well controlled [16-18].

The aim of this paper is to present the results of the synthesis of ZnGa_2O_4 nanoparticles by the hydrothermal method using Ga_2O_3 , $\text{Zn}(\text{NO}_3)_2 \cdot 6\text{H}_2\text{O}$ and Er_2O_3 .

2. Experimental procedure

For obtaining of $\text{ZnGa}_2\text{O}_4:\text{Er}^{3+}$ nanocrystalline samples by hydrothermal method we used $\text{Zn}(\text{NO}_3)_2 \cdot 6\text{H}_2\text{O}$, Ga_2O_3 and Er_2O_3 as reactants, with molar ratio Zn:Ga of 1:2. The resulting mixture was then adjusted to a special pH=12 with sodium hydroxide solution under vigorous stirring. The resulting suspension was transferred into a Teflon-lined stainless steel autoclave and sealed tightly and was introduced in an oven at 210°C for 4 h. It results a white precipitate that was filtrated and washed for many times with distilled water and ethylic alcohol, then dried in oven at 105°C for 4hours. After drying was achieved characterization of obtained material by X-ray diffraction (XRD) on an X'pert Pro MPD X-ray diffractometer, with monochromatic $\text{Cu K}\alpha$ ($\lambda = 1.5418 \text{\AA}$) incident radiation. Regarding identification of the morphology, dimension and composition of the sample was used field emission-scanning electron microscopy (SEM; Model INSPECT S), energy dispersive spectroscopy (EDAX) and atomic force microscopy (AFM; Model Nanosurf easy Scan). The photoluminescence (PL) measurement was carried out by using spectrofluorophotometer at room temperature. Was used a xenon lamp 150 W as the excitation source.

3. Results and discussion

3.1 X-ray diffraction

Hydrothermal method is a success method regarding nanomaterials obtaining with a high degree of crystallinity and also homogeneity of particle's size.

Fig. 1 shows the XRD patterns of $\text{ZnGa}_2\text{O}_4:\text{Er}^{3+}$ samples obtained from Ga_2O_3 , $\text{Zn}(\text{NO}_3)_2 \cdot 6\text{H}_2\text{O}$ and Er_2O_3 by hydrothermal method of at 210°C for 4 h.

It is seen from the form of the peaks in the XRD pattern that the $\text{ZnGa}_2\text{O}_4:\text{Er}^{3+}$ spinel particles have a high degree of crystallinity.

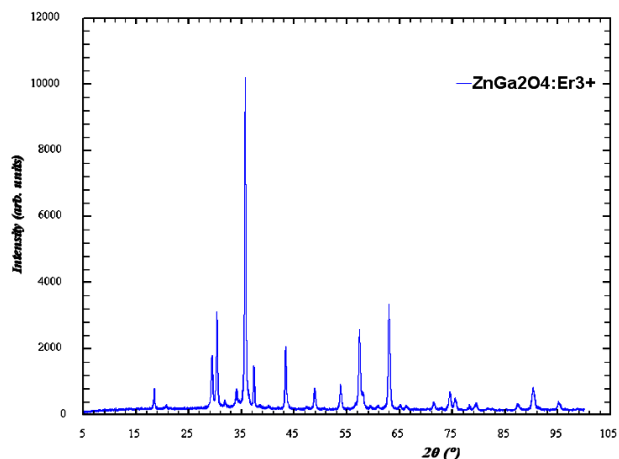


Fig. 1. XRD patterns of $\text{ZnGa}_2\text{O}_4:\text{Er}^{3+}$ samples obtained by hydrothermal method.

3.2 SEM- analysis

The SEM image shown in Fig. 2 provides direct information about size and morphology type of the $\text{ZnGa}_2\text{O}_4:\text{Er}^{3+}$ compound obtained by hydrothermal method.

By SEM images we can observe that particles have oblong form (bars) and dimension between 600-900 nm.

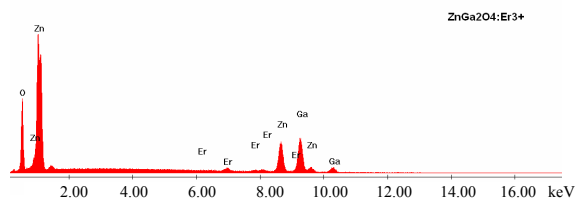
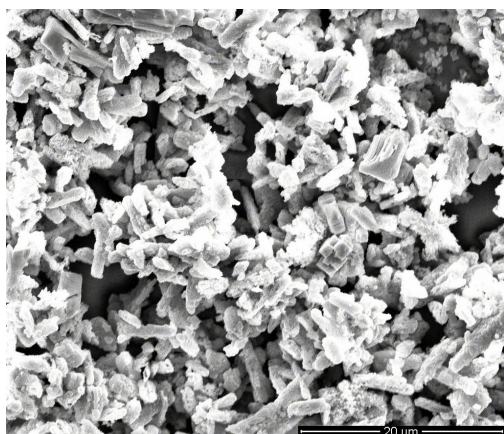


Fig. 2. SEM image of $\text{ZnGa}_2\text{O}_4:\text{Er}^{3+}$ compound obtained by hydrothermal method. The qualitative EDAX analysis.

3.3 AFM- analysis

Fig. 3. shows AFM surface morphology of $\text{ZnGa}_2\text{O}_4:\text{Er}^{3+}$ obtained by hydrothermal method. The roughness and surface morphology of the $\text{ZnGa}_2\text{O}_4:\text{Er}^{3+}$ thus obtained by hydrothermal method are different according to autoclavation conditions.

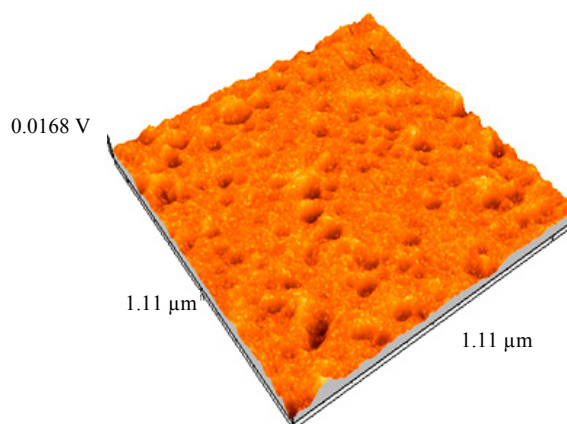


Fig. 3. AFM image of $\text{ZnGa}_2\text{O}_4:\text{Er}^{3+}$ obtained by hydrothermal method.

3.4 Photoluminescence

The luminescence characteristic of the samples obtained by hydrothermal method from different precursors is studied.

Fig. 4 presents the room temperature emission spectra of all the samples under excitation at 1550 nm. The emission spectrum of all the samples shows a broad-band emission, but the maximum emission peak and intensity are different. The $\text{ZnGa}_2\text{O}_4:\text{Er}^{3+}$ phosphors obtained from Ga_2O_3 , $\text{Zn}(\text{NO}_3)_2 \cdot 6\text{H}_2\text{O}$ and Er_2O_3 emit lower intensity light.

The photoluminescence (PL) of the prepared $\text{ZnGa}_2\text{O}_4:\text{Er}^{3+}$ films in infrared region were observed at room temperature. A main peak centered at 1550 nm. The peak centered at 1550 nm should originate from the transition between the first excited state ($^4\text{I}_{13/2}$) and the ground state ($^4\text{I}_{15/2}$) in the Er^{3+} ions.

Through the previous study of optically active center in Er-doped $\text{ZnGa}_2\text{O}_4:\text{Er}^{3+}$ by EDAX analysis, we acknowledge that the variance in the bonding state of Er-O, the local structure uniformity and the effects of the crystal field of $\text{ZnGa}_2\text{O}_4:\text{Er}^{3+}$ are the key parameters that influence the emission at 1.55 μm of Er doped semiconductor. Concerned with the macrostructure of the sample, the XRD results showed the crystal quality of the four samples were improving with the increasing of the annealed temperatures, which can lead to the enhancement of the mobility of the excited carriers in $\text{ZnGa}_2\text{O}_4:\text{Er}^{3+}$. Consequently, the local structure around Er probably forms a similar pseudo-octahedron with C_{4v} point structure as described in [19, 20, 21]. The improvement of crystal quality of $\text{ZnGa}_2\text{O}_4:\text{Er}^{3+}$ and the formation of proper

oxygen-octahedron around Er lead to the strongest emission at 1550 nm for the films annealed at 240°C. Consequently, the Er active center reduced and the mobility of the excited carriers weakened. We notice that there is no evidence of the existence of the crystalline fragment related with either Er₂O₃ or Er–O system in XRD. We emphasize this fact for the consideration of the PL emission mechanism of our Er-doped ZnGa₂O₄:Er³⁺ system.

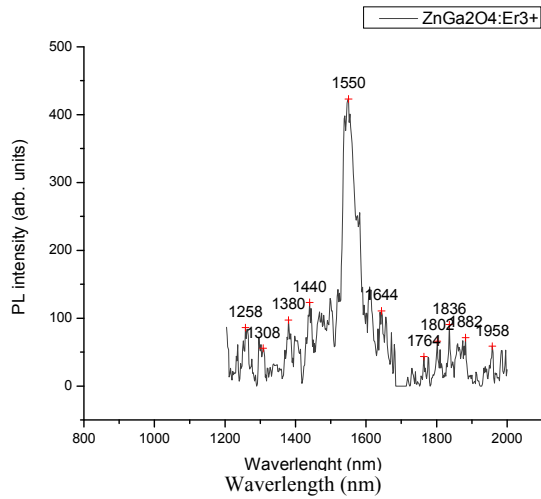


Fig.4. Photoluminescence spectra of the samples obtained by hydrothermal method.

Tentative scheme for energy levels

The experimental supports for our calculation are the obtained results for nanocrystal ZnGa₂O₄ doped with erbium trivalent ion. Er³⁺ substitutes the Ga³⁺ ion and has an octahedral coordination of O²⁻ ions with local site symmetry.

The free-ion states of a rare earth ion are composed of linear combinations of Russell-Saunders states which are found by diagonalizing the combined electrostatic and spin-orbit energy matrices. The effect of the host's Stark field reduces the (2J+1)-fold degeneracy of the free-ion states and causes a small admixing of states. Because the effect of the field on the 4f^N configuration is small it is treated as a perturbation of the free-ion states.

Electrical charges of both substituted and substituting ions are the same; no compensating addition is required to keep electrical neutrality of the crystals.

The measured energy spectrum of Er³⁺ ions in ZnGa₂O₄ was analyzed using the Hamiltonian:

$$H = H_{FI} + H_{CF} \quad (1)$$

where H_{FI} is the effective free-ion Hamiltonian,

$$H_{FI} = \sum_{k=0,2,4,6} F^k f_k + \xi_{nl} A_{so}(nl) + \alpha L(L+1) + \beta G(G_2) + \gamma G(G_7) + \sum_{i=2,3,4,6,7,8} T^i t_i + \sum_{i=0,2,4} M^i m_i + \sum_{i=1,4,6} p_i P^i \quad (2)$$

The electrostatic interaction between 4f electrons determined by Racah parameters F^2 , F^4 , F^6 , spin-orbit interaction (with the coupling constant ζ), Trees' two-particle (α , β , γ parameters) and Judd' three-particle (parameters $T^2 - T^4$, $T^6 - T^8$) corrections to the electrostatic interaction were taken into account in the free-ion Hamiltonian. For Er³⁺ ions the parameters are: $F^2=97483$, $F^4=67904$, $F^6=54010$, $\alpha=1779$, $\beta=-582.1$, $\gamma=1800$, $\zeta=2376$, $T^2=400$, $T^3=43$, $T^4=73$, $T^6=-271$, $T^7=308$, $T^8=299$, $M^0=3.86$, $M^2=2.16$, $M^4=1.19$, $P^2=594$, $P^4=297$, $P^6=59.4$, $\sigma_2=127$. H_{CF} corresponds to the interaction of the Er³⁺ ground 4f¹¹ configuration with the crystal field.

The Hamiltonian of 4f¹¹ electrons of the Er³⁺ ions in a crystal field may be expressed in terms of Stevens equivalent operator under trigonal symmetry [22].

$$H = B_2^0 O_2^0 + B_4^0 O_4^0 + B_4^3 O_4^3 + B_6^0 O_6^0 + B_6^3 O_6^3 + B_6^6 O_6^6 \quad (3)$$

In order to calculate the crystal field parameters B_k^q in Eq. (3) the superposition model [23] is adopted, i.e.,

$$B_k^q = \sum \bar{A}_k(R_0) \left(\frac{R_0}{R_j} \right)^{t_k} K_k^q(\theta_j, \varphi_j) \quad (4)$$

where the coordination factor can be expressed by using the structural parameters of the studied system. $\bar{A}_k(R_0)$ and t_k are, respectively, the intrinsic parameters and the power law exponents. For the [ErO₆]⁹⁻ cluster, the intrinsic parameters

$$\bar{A}_2(R_0) \cong 1030 \text{ cm}^{-1}, \bar{A}_4(R_0) \cong 127.1 \text{ cm}^{-1}, \bar{A}_6(R_0) \cong 22.1 \text{ cm}^{-1}$$

(with the reference distance $R_0=0.21$ nm) and the power-law components $t_2=3.4$, $t_4=7.3$ and $t_6=2.8$ were obtained for MgO:Er³⁺ crystal [24]. They can also be approximately applied in similar [ErO₆]⁹⁻ clusters in ZnGa₂O₄:Er³⁺. The work is in progress.

In Table 1 we give the calculated values of the energy levels for Er³⁺ free ion and assignments of experimental values for Er³⁺ doped in ZnGa₂O₄.

Table 1. Energy levels (in cm⁻¹) of free Er³⁺ ion and Er³⁺ ion in ZnGa₂O₄.

Energy levels	This work	
	Free ion	Experimental Er ³⁺ :ZnGa ₂ O ₄
⁴ G _{11/2}	25929	7949
² H _{9/2}	23874	7645
⁴ F _{3/2}	21978	7246
⁴ F _{5/2}	21733	6944
⁴ F _{7/2}	20034	6451
² H _{11/2}	18851	6082
⁴ S _{3/2}	18018	5668
⁴ F _{9/2}	14913	5549
⁴ I _{9/2}	12003	5446
⁴ I _{11/2}	10043	5313
⁴ I _{13/2}	6511	5107
⁴ I _{15/2}	0	0

4. Conclusions

ZnGa₂O₄ powders were synthesized by the hydrothermal method using as reactants Ga₂O₃, Zn(NO₃)₂·6H₂O and Er₂O₃. The reactant concentration and reaction medium have a particularly importance regarding hydrothermal synthesis. The X-ray diffraction shows a high crystallization degree for ZnGa₂O₄:Er³⁺. SEM analyses suggest that particles have oblong form and dimension between 600-900 nm. The assignments of luminescent spectra to crystal field levels are given and a tentative to modulation of this energy levels have made.

References

- [1] M. Wendschuh-Josties, H. S. C. O'Neill, K. Bente, G. Brey, Neues Jahrbuch für Mineralogie Monatshefte, **6**, 273, (1995);
- [2] I. I. Krebs, G. H. Stauss and I. B. Milstei, Phys. Rev. **B20**, 2586 (1979);
- [3] S. Itoh, H. Toki, Y. Sato, K. Morimoto, T. Kishino, I. Electrochem. Soc., **138**, 1509 (1991).
- [4] J. S. Kim, J. S. Kim H. L. Park, Solid State Commun **131**, 735 (2004).
- [5] M. Yu, Y. H. Zhon, S. B. Wang, Mater. Lett. **56**, 1007 (2002).
- [6] J. S. Kim, I. S. Kim, T. W. Kim, S. M. Kim, H. L. Park, Appl. Phys. Lett. **86**, 091912 (2005).
- [7] T. Ohtake, N. Sonoyama, T. Sakata, Chem. Phys. Lett. **318**, 577 (2000).
- [8] P. D. Rack, I. I. Peterson, M. D. Potter, W. Park, I. Mater, Res. **16**, 1429 (2001).
- [9] T. K. Tran, W. Park, J. W. Tomm, B. K. Wagner, S. M. Jacobsen, C. J. Summers, P. N. Yocom, S. K. McClelland, J. Appl. Phys. **78**, 6591 (1995).
- [10] S. K. Sampsth, J. F. Cordaro, J. Am. Ceram. Soc. **81**, 649 (1988)
- [11] T. Omata, N. Ueda, H. Kawazoe, Appl. Phys. Lett. **64**, 1077 (1994).
- [12] Z. Yan, H. Takei, J. Cryst, Growth **171**, 131 (1997).
- [13] Z. Yan, H. Takei, H. Kawazoe, J. Am. Ceram. Soc. **81**, 180 (1998)
- [14] L. Chen, Y. Liu, Y. Li, J. Alloy Compd. **381**, 266 (2004).
- [15] Z. Lu, Y. Tang, L. Chen, Y. Li, J. Cryst. Growth **266**, 539 (2004).
- [16] X. Wang, Y. Li, J. Am. Chem. Soc. **124**, 2880 (2002).
- [17] Y. Li, J. Wang, Z. Deng, J. Am. Chem. Soc. **123**, , 9904 (2001).
- [18] X. Li, J. Liu, Y. Li, Appl. Phys. Lett. **81**, 4832 (2002).
- [19] M. Ishii, S. Komuro, T. Morikawa, Y. Aoyagi, J. Appl. Phys **89**, 3679 (2001).
- [20] M. Ishii, T. Ishikawa, T. Ueki, S. Komuro, T. Morikawa, Y. Aoyagi, H. Oyanagi, J. Appl. Phys. **85**, 4024 (1999).
- [21] M. Ishii, S. Komuro, T. Morikawa, Y. Aoyagi, T. Ishikawa, T. Ueki, Jpn. J. Appl. Phys. Suppl. **38**, 191 (1999).
- [22] A. Abragam, B. Bleaney, Electron Paramagnetic Resonance of transition Ions, University Press, London, 1970.
- [23] D. I. Newman, W. Urban, Adv. Phys. **24**, 793 (1975).
- [24] S. C. Chen, D. I. Newman, J. Phys. **C17**, 3045 (1984).

*Corresponding author: avram@physics.uvt.ro